machines

MDPI

Article

Material Extrusion 3D Printing of Micro-Porous Copper-Based Structure for Water Filters

Nikola Kotorčević [1], Strahinja Milenković [1], Fatima Živić [1,*], Branka Jordović [2], Dragan Adamović [1], Petar Todorović [1] and Nenad Grujović [1]

[1] Faculty of Engineering, University of Kragujevac, 34000 Kragujevac, Serbia; nikola.kotorcevic@uni.kg.ac.rs (N.K.); strahinja.milenkovic@fink.rs (S.M.); adam@kg.ac.rs (D.A.); petar@kg.ac.rs (P.T.); gruja@kg.ac.rs (N.G.)
[2] Engineering Academy of Serbia, 11000 Belgrade, Serbia; branka.jordovic46@gmail.com
* Correspondence: zivic@kg.ac.rs

Abstract: This paper presents 3D-printed micro-porous structures made of a Cu/PLA composite by using material extrusion 3D printing technology. A metallic filament made of 80% copper and 20% polylactic acid (PLA) was used for the 3D printing of the porous samples. We varied printing parameters, aiming to obtain a micro-range porosity that can serve as a water-filtering structure. The produced samples were analyzed from the aspects of dimensional accuracy, level of porosity, and capacity for water flow. Several samples were fabricated, and the water flow was exhibited for the samples with an approximate 100 μm size of the interconnected open porosity. The application of material extrusion 3D printing, as a cost-effective, widely available technology for producing micro-range porous structures, is still challenging, especially for interconnected predefined porosity with metal-based filaments. Our research showed that the optimization of 3D printing parameters can enable the fabrication of copper-based micro-porous structures, but further research is still needed.

Keywords: metal additive manufacturing; material extrusion 3D printing; copper (Cu); polylactic acid (PLA); nature-based material; antibacterial filter; water filter

Citation: Kotorčević, N.; Milenković, S.; Živić, F.; Jordović, B.; Adamović, D.; Todorović, P.; Grujović, N. Material Extrusion 3D Printing of Micro-Porous Copper-Based Structure for Water Filters. *Machines* **2024**, *12*, 470. https://doi.org/10.3390/machines12070470

Academic Editor: Swee Leong Sing

Received: 29 April 2024
Revised: 1 June 2024
Accepted: 9 July 2024
Published: 12 July 2024

1. Introduction

Material extrusion 3D printing technology, according to ISO/ASTM terminology, or Fused Deposition Modeling (FDM, trademarked acronym from Stratasys 3D printers) [1], is a widely available 3D printing technology whereby filament is extruded through a heated nozzle and deposited on a build plate in subsequent layers, thus creating 3D-printed objects. The optimization of printing parameters still represents a challenge [2–4], as does dimensional accuracy, especially in relation to composite filaments [5]. Pure polylactic acid (PLA), as a nature-based, eco-friendly material, is among the most widely used filament materials, but its mechanical properties still limit final applications, and different material extrusion 3D printing optimization techniques have been studied [6]. Filaments made of natural materials are of great significance for sustainable materials in different areas [7]. PLA also serves in combinations (blends or composites) with different materials, from other polymers to metallic materials such as copper (Cu) [8,9], with applications in filtration systems [10,11], electronics [12], and the biomedical field [13].

Reinforcing PLA with other materials has a profound effect on the filament's mechanical properties, and further on the properties of the printed objects [11,14], whereas a PLA/Cu composite is influenced by PLA's brittleness upon impact [15]. Copper as a PLA reinforcement significantly improves the flexural strength and flexural modulus [16] and increases yield strength [15]. Copper-based filaments have good corrosion resistance, thermal and electrical conductivity, and also exhibit antibacterial properties [5]. Pure copper and copper-based materials have excellent antiviral and antibacterial properties in relation

to a wide group of pathogens and viruses [17]. Composites with 90% copper and 10% PLA also show high antibacterial properties [18].

Processing parameters during the material extrusion 3D printing process, such as printing temperature and speed, as well as filament orientation, essentially affect the final material properties of the printed objects. Printing orientation and layer thickness have been shown to have a significant impact on compressive strength [19]. Variation in the printing temperature has effects on the bonding between PLA and copper and can result in random small voids that also further influence the mechanical properties of the printed object [19]. On the other hand, the fabrication of the designed porosity within 3D-printed objects is very significant for a range of applications, including water filters. Cu/PLA filaments have been used for 3D-printed porous structures where the desired porosity was finally achieved through thermal post-processing that removed the polymer component to produce pure copper foam [20].

Water purification, especially of wastewater, is one of the most pressing issues of modern society, and sustainable materials are desired in these systems [21,22]. Antimicrobial water filters made of 3D-printed PLA have been studied, including methods to improve the ability of PLA to destroy pathogens [23]. Three-dimensional-printed, biobased water filters are a significant topic of research, focusing on nature-based materials in different types of composites that can provide ion adsorption, the removal of micro-organisms from water, and microplastic separation while also considering the suitable mechanical properties of these materials to provide adequate functional durability [24,25]. PLA-based composites have also been studied for heavy metal removal from water [21].

Pure copper filters have been used as reusable filters in face masks to fight the COVID-19 virus [26,27], for water purification [28,29], air filtration [30–32], and for oil−water separation [33,34]. Pure copper filters have shown high efficiency in water purification, in correlation with porosity and wetting properties [28]. The application of copper filters has wide potential, from antibacterial effects [26], the purification of drinking water, wastewater treatments [28], and oil manipulation underwater to the support of self-cleaning and bioadhesion control [34]. Porous copper filters have been produced from powders by hydraulic pressing [30] and cold isostatic pressing [31], by using the electrodeposition of copper dendrites to produce nanostructured porous filters [32] and through the laser treatment of copper sheets [33–35].

A combination of copper and PLA in a porous Cu/PLA composite structure [20] could be used for different water filters. The Cu/PLA composite has exhibited improved properties [15], especially important from the aspects of the functional durability of pure water filters or wastewater filters. In copper-based composites, one of the significant challenges is the agglomeration of Cu particles which makes it hard to produce composites with a homogeneous distribution of the copper phase. Polymers have been used to form a coating around Cu particles to prevent agglomeration, like in polyethylene glycol (PEG)/Cu composites [36]. However, recent EU legislation demands the replacement of traditionally used polyolefin-based polymers (e.g., polyethylene, PE, polypropylene, PP, or polyethylene terephthalate, PET) with sustainable and green polymers such as biodegradable and biobased PLA [37]. The PLA price is decreasing, bringing it closer to the cost of PE- or PP-based polymers that have been the major industrially produced polymer materials for a wide range of applications.

PLA and copper particles can be mixed to form a composite Cu/PLA filament by the extrusion process, under elevated temperatures (approx. 200 °C) [36]. The material extrusion 3D printing of pure copper at this temperature range is impossible, considering its sintering temperature range of 750–1000 °C. The addition of PLA acts as a binder for copper particles in a Cu/PLA composite filament, thus enabling the use of this low-cost 3D printing technology for the fabrication of complex porous filters made of both Cu-based composites and pure copper since it is relatively easy to remove PLA from a 3D-printed object through post-processing, especially considering PLA biodegradability. Another advantage of selecting PLA for the Cu/PLA composite in our research is the possibility of

the wider application of such filters beyond water treatments and further in biomedical and food-packaging products, since PLA is an FDA (U.S. Food and Drug Administration)-approved biomaterial in both areas. PLA-based filaments for material extrusion 3D printing commonly do not use Bisphenol-A (BPA) in the manufacturing process, like other traditional polymers. Hence, they are BPA-free, which is a very significant property for food products. Furthermore, it has been studied for use in personal protective equipment to replace single-use filters [38]. The production of PLA requires approx. 65% less energy than traditionally used polymers, with 68% lower emissions of greenhouse gases [37]. PLA is not fully waterproof and exhibits swelling and water absorption over longer periods of time; thus, further research is needed for the water filter application. PLA is UV-resistant with heat resistance to approx. 60 °C Tg (glass transition temperature) [39]. PLA should not generate toxic microplastics, as one of the major concerns today, since PLA microplastics would represent biocompatible and environmentally friendly particles that should naturally degrade with time, but there are no comprehensive research data related to those aspects. Data from the use of 3D-printed consumer products indicate that PLA will not rapidly degrade, except in the presence of organic solvents (e.g., benzene or chlorinated solvents) [36].

In this paper, we used material extrusion 3D printing with Cu/PLA filaments, made of 80% copper and 20% PLA, to fabricate micro-porous structures with open porosity. We studied the influence of the printing parameters on porosity level and the ability to predefine the shape and size of the pores. Also, water flow ability through these copper-based porous structures was studied, aiming to create structures that can be used in water filters.

2. Materials and Methods

A metal filament made by PrimaSelect (Malmö, Sweden), with 80% copper and 20% PLA, was used for material extrusion 3D printing with a CR-10 S5 printer (Shenzhen, China). UltiMaker Cura software, version 5.5.0, was used for CAD and STL file design. The diameter of the filament was 1.75 mm, and specific gravity was 3.59 g/cm^3. Rectangular samples with dimensions of 10 mm × 10 mm× 3 mm were printed for further analysis. Eight different test samples were made, with varying printing parameters: linear distance, nozzle temperature, and build plate temperature, as shown in Table 1. Three-dimensional printing parameters were varied until micro-porosity was obtained. The objective was to print porous, copper-based samples with micro-porosity that would allow for water flow. The Taguchi method was used for the design of the experiment, with an L8 array with 3 factors, and levels and factors were defined in the Minitab software, version 22.1.

Table 1. Material extrusion 3D printing parameters for eight different test samples.

Sample	Linear Distance [mm]	Nozzle Temperature [°C]	Build Plate Temperature [°C]
1	0.4	210	60
2	0.4	210	70
3	0.4	220	60
4	0.4	220	70
5	0.5	210	60
6	0.5	210	70
7	0.5	220	60
8	0.5	220	70

Samples were studied by using optical and SEM microscopy (SEM FEI Scios2 Dual Beam System, Waltham, MA, USA). A custom setup was used for the testing of the fluid flow, as shown in the next chapter. A universal mechanical tester (Brookfield CT3, Harlow,

Essex, UK) was used to measure the load applied during fluid flow tests, with a water-filled syringe with the sample fit inside. For each sample, the test was repeated three times. We measured the applied load and time (duration of the compression). The speed of the tool was 0.1 mm/s, and the compressing distance was 15 mm for the maximum traveling path of the compressing tool.

An additional set of round samples was fabricated to test the water flow ability. The fluid flow was tested on all samples (Table 1), printed as round samples (20 mm diameter and 3 mm height) that were firmly fitted inside a syringe cylinder of 20 mL.

According to the ISO 5167–1:2022 standard, the volume flow rate (q_V) is defined as the volume of fluid (V) passing through the primary device per unit time (t) [40]:

$$qv = V/t \quad (1)$$

For comparison, the water flow test was also performed with the 3D-printed sample with the following printing parameters: infill line distance 0.3 mm, printing temperature 210 °C, and build plate temperature 60 °C, which resulted in a solid sample with no porosity or a very low closed-porosity structure, thus preventing the water flow through it.

Sample porosity (%T.P.) was determined by using the Archimedes principle. Analytical balance RAD WAG AS 220.R2 (Radom, Poland) was used to measure the mass of the test sample (m); the mass of the calibrated measuring cup filled with distilled water (m_1); and the mass of the calibrated measuring cup filled with distilled water with the test sample inside (m_2), both with the same volume setup. The density of distilled water is known ($\varrho_0 \approx 1$ g/cm^3), and the density of the Cu/PLA filament was given by the manufacturer ($\varrho_{Cu/PLA} \approx 3.6$ g/cm^3). Hence, the density of the sample (ϱ), theoretical density (%T.D.), and total porosity (%T.P.) can be calculated by using the following equations [41]:

$$\varrho = \varrho_0 \cdot m/(m_1 - m_2) \quad (2)$$

$$\%T.D. = (\varrho/\varrho_{Cu/PLA}) \times 100 \quad (3)$$

$$\%T.P. = 100 - \%T.D. \quad (4)$$

3. Results and Discussion

We fabricated samples with different levels of porosity depending on the printing parameters (Table 1), as shown in Table 2. Higher values of porosity can be observed in test samples 5–8, as expected due to the higher linear distance between the filaments that were set up during printing. Our results showed that we can expect a reasonable repeatability of the porosity level depending on the 3D printing process parameters. The linear distance parameter showed the most significant influence, as expected, but other process parameters also influenced the resulting level of porosity and material structure.

Table 2. The porosity of 3D-printed samples depending on the printing parameters.

Sample Number	Sample Mass, m [g]	Density of Sample, ϱ [g/cm^3]	Percentage of Theoretical Density, %T.D. [%]	Percentage of Total Porosity, %T.P. [%]
1	0.906	1.759	48.874	51.126
2	0.895	1.665	46.253	53.747
3	0.988	1.845	51.253	48.747
4	0.894	1.785	49.592	50.408
5	0.679	1.188	32.988	67.012
6	0.682	1.370	38.058	61.942
7	0.689	1.335	37.094	62.906
8	0.685	1.556	43.222	56.778

Samples were analyzed by optical microscopy that showed porosity with no significant defects. A comparison between test samples 1 and 5 is shown in Figure 1. Larger pore sizes can be observed in samples with higher values of linear distance during printing. This was to be expected, since higher values of linear distance during printing resulted in higher porosity, as shown in Table 2. Nozzle temperature, build plate temperature, and printing speed did not show a significant influence on the pore size or level of porosity.

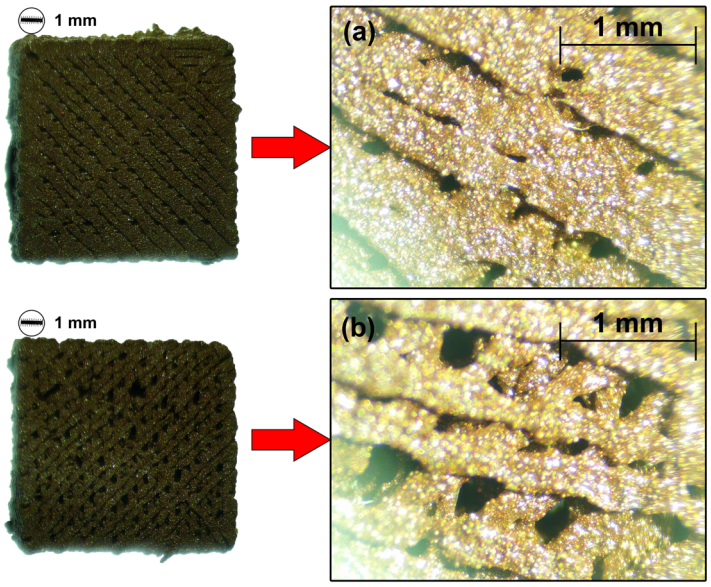

Figure 1. Comparison of sample 1 and sample 5 from aspect of pore sizes: (**a**) sample 1 and (**b**) sample 5.

SEM images of the selected samples are shown in Figure 2, where voids in the structure can be clearly seen, thus showing that a micro-porous structure was fabricated by material extrusion 3D printing. Similar structures were also observed in other samples. However, since SEM microscopy shows only a surface view, porosity could be closed in some regions throughout the sample volume, even though the higher porosity levels (Table 2) indicate that this should not be the case. Therefore, additional water flow tests were performed with samples that had the lower calculated porosity level (sample 1, Table 2), also in comparison to the sample with no porosity, as explained in the previous Materials and Methods Section. These two samples are shown in Figure 3. The custom test setup for the water flow test is shown in Figure 4.

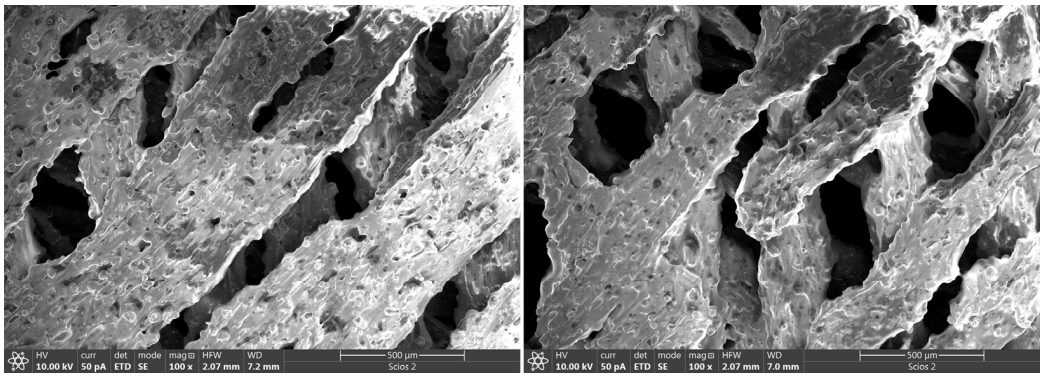

Figure 2. SEM images of the test samples: sample 1 (**left image**) and sample 5 (**right image**).

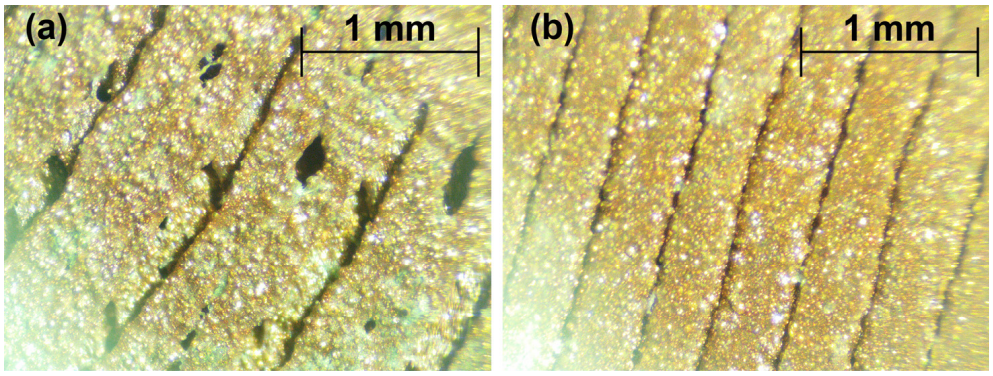

Figure 3. Samples for water flow tests: (**a**) with open porosity (sample 1) and (**b**) sample fabricated without porosity.

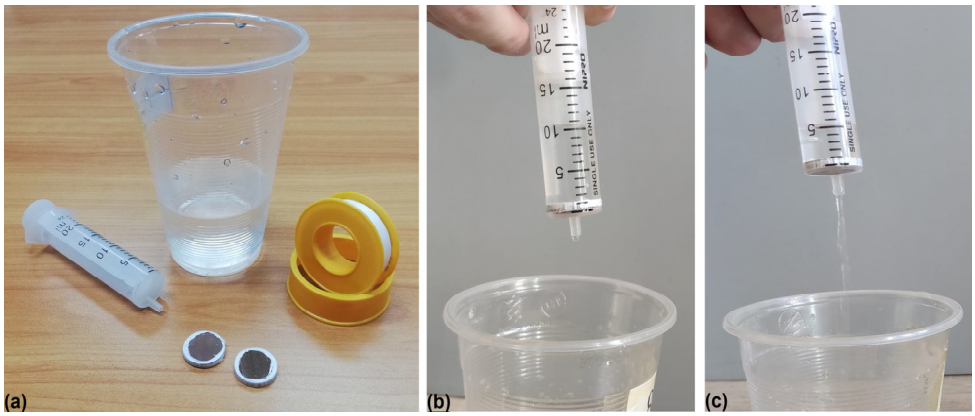

Figure 4. Custom setup for water flow tests: (**a**) water container, test samples, syringe, PTFE tape; (**b**) suspended water flow with the sample with a non-porous structure (Figure 3b); (**c**) water flow through a filter with a porous structure (Figure 3a).

Samples were fitted inside the syringe and filled with water, and water was compressed through it afterwards. PTFE tape was used to seal the edges of the sample to prevent water flow around the sample edges, even though a few drops of water were noted to pass around the tape in the case of the non-porous sample test (Figure 3b). Strong water flow was observed in the case of the porous sample (sample 1, Figure 3a), thus indicating fully open porosity through the sample volume. Further research will use a more sophisticated test setup to analyze the water flow in detail. Moreover, the pressure needed to start the water flow was significantly lower in the case of the porous samples compared to the high pressure applied for the non-porous sample that did not produce water flow. Accordingly, we analyzed the compressive load by using the mechanical tester and custom-made holder of the water-filled syringe, thus measuring precisely the value of the required load.

Further tests were conducted with porous samples to determine the load. A custom-made holder of the syringe was used to position it at the mechanical tester to measure the compressive load during the compression of the syringe plunger, with a constant speed of 0.1 mm/s. In the case of the non-porous structure, the results are shown in Figure 5, with the load continuously increasing up to the average maximum of 44 N over the whole distance.

Compressive tests with porous samples showed a slight difference in the maximum load, as shown in Figure 6, for all samples, where each of the curves was obtained from the average values of three measurements for each of the samples.

It was observed that after the start of the compression, the load reached the maximum value, which is almost four times lower than in the case of the non-porous sample. The water flow started almost immediately and continued until the end of the compressing

distance (15 mm). After a rapid initial load increase and reaching the maximum value, the load was almost constant until the end of the test, thus indicating stable water flow.

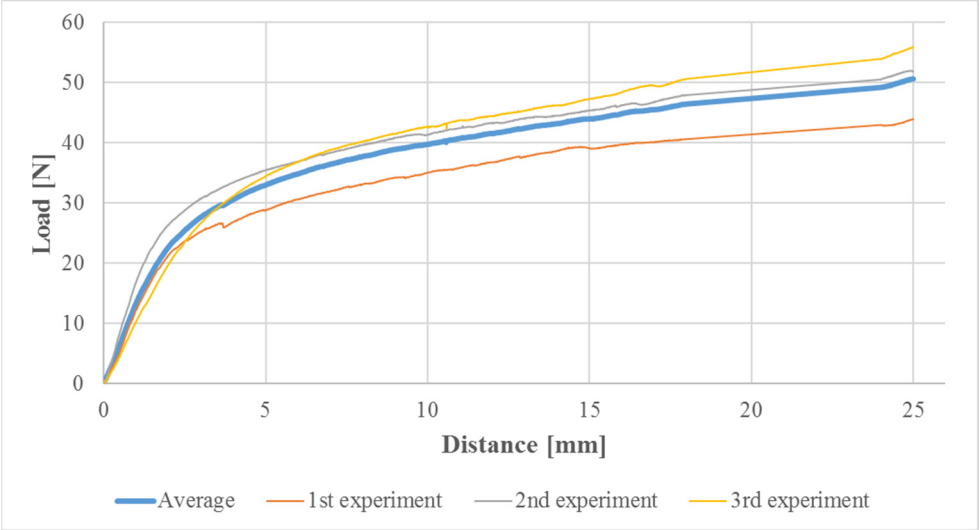

Figure 5. Load change during compressive water flow test with non-porous sample (Figure 3b).

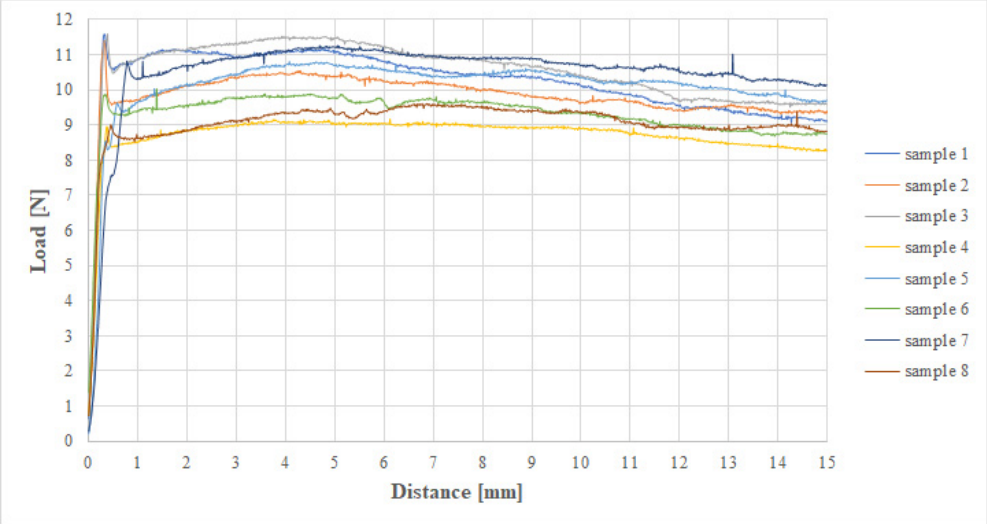

Figure 6. Load change during compressive water-flow test with porous samples 1–8 (Table 1).

The maximum loads were between 9.2 N (sample 4) and 11.6 N (sample 3). According to these results, there are no significant differences in the shapes of the curves (Figure 6) for all samples with very low differences in the maximum load required for water flow through different porous samples. It can be concluded that the printing parameters for the fabrication of samples 1–8 resulted in a porous structure, since the maximum load to produce a water flow is significantly lower in comparison to the non-porous sample.

Volume flow rate was calculated using Equation (1). The volume of the water was calculated from the following Equation (5):

$$V = r^2 \cdot \pi \cdot h \quad (5)$$

where the radius (r) of the syringe cylinder is known (10 mm), and the height (h) of the cylinder is determined by the maximum traveling distance of the compression tool (15 mm). The universal mechanical tester provided the load values and duration of the compression test (approximately 149 s for each sample), with a travel tool speed of 0.1 mm/s.

Accordingly, the constant volume flow rate value was calculated to be 3.2×10^{-8} m^3/s for all test samples. Different loads were required to reach this constant flow rate for each of the samples.

Pure PLA is brittle, with approximately 60 MPa ultimate tensile strength value (UTS) [42,43]. Pure copper has a UTS value of 175 MPa [44]. The glass transition temperature of PLA is around 60 °C [39]. Composites with a PLA matrix and copper particle reinforcements decrease UTS in comparison to the pure PLA [15,36,40–42], due to an increase in voids within the structure around the particle reinforcements [45]. On the other hand, the presence of copper particles improves the values of the Young's modulus of the composite in comparison to pure PLA [45–47]. Significant differences in the mechanical properties of PLA and copper can result in rather different values for the Cu/PLA composite's properties, depending on the processing parameters [48]. The post-processing of 3D-printed samples can provide improvements in mechanical properties [47,49]. Also, printing parameters have a significant influence on the final mechanical properties of the printed composites [50]. Smaller voids and pits can be seen in Figure 2, which is consistent with the literature [51]. Some authors have pointed out that regions with small voids within the composite structure contribute to good layer adhesion during material extrusion 3D printing [52]. Considering the different mechanical properties of copper and PLA, we can elaborate that the small pits that can be seen in Figure 2 originated and developed in the PLA matrix, since the printing temperatures have no influence on the copper phase.

We fabricated a micro-porous Cu/PLA composite structure with a pore size of approximately 100 μm, as can be seen in Figure 2, which is in accordance with other research results regarding micro-scale structures produced by additive manufacturing [53–56]. Pure copper structures of 400 nm size were fabricated by 3D electrohydrodynamic redox printing [57]. Material extrusion 3D printing was used to fabricate polymer structures of approx 100 μm size [58]. A further post-processing of 3D-printed samples should enable finer adjustments of pore size, in addition to the possibility to influence its mechanical properties.

We showed that material extrusion 3D printing, as a cost-effective, widely available technology, can be used for the fabrication of custom-designed micro-porosity in copper-based filters. However, further research is needed to gain insights into the dependencies between the final material properties and the water filtration ability, as well as the fine-tuning of 3D printing parameters to produce customized shapes of interconnected pores. Additionally, possible material combinations in composites, through custom-made, copper-based filaments, which can enable efficient water purification from different aspects, need to be studied.

The objective of our research was to produce micro-porous Cu/PLA structures aimed at water filters. Hence, future research will include the fine-tuning of the size, shape, and distribution of pores and the correlation to the mechanical properties of the printed porous samples and functional behavior under external influences in wet environments such as water-based solutions and suspensions. Dependencies between the final material properties and the water filtration ability, including more detailed water flow analysis, will be conducted. Methods to improve the dimensional accuracy of material extrusion 3D printing will be studied through the comparison of experimentally obtained porosity levels and planned porosity from the input CAD files to 3D printing. The post-processing of the fabricated samples will be studied to improve the mechanical properties of the Cu/PLA composite, such as laser polishing to provide an improved storage and loss modulus, glass transition temperature, and strength. Furthermore, mechanisms related to water purification will be studied, from the aspects of existing water pollutants, such as microorganisms, or material behavior and the durability during water flow and higher water pressures, including the mechanical properties of porous structures under such complex loading conditions. Also, possibilities to produce pure copper micro-porous filters for wider applications, by removing the polymer component from the composite through post-processing, will be further investigated.

4. Conclusions

We have fabricated different samples of porous structures made of a Cu/PLA composite with a predefined size of micro-porosity, by using cost-efficient material extrusion 3D printing technology. Our results showed that a combination of printing parameters can produce customized porosity aimed at copper-based filters. It is still challenging to produce a predefined shape and size of micro-range porosity due to dimensional variations that depend on the filament material, as well as process parameters and machine errors. Small variations in the printing parameters can produce closed porosity that can completely stop the water flow, as shown in our paper. The lack of widely available metal filament materials represents yet another challenge that can be overcome by the fabrication of customized filaments at the site, which will be the future direction of our research. However, different properties of the copper powder to be used for metal filaments should also be further studied, including the mechanical properties of such printed filters. In general, material extrusion 3D printing (or commonly known as FDM 3D printing) is a promising technology for the low-cost fabrication of water filtration solutions.

Author Contributions: Conceptualization, N.K., S.M. and F.Ž.; methodology, N.K. and S.M.; validation, F.Ž., N.G., D.A. and P.T.; formal analysis, N.K., S.M. and B.J.; investigation, N.K., S.M., F.Ž., B.J., D.A., P.T. and N.G.; resources, F.Ž.; data curation, N.K., S.M. and F.Ž.; writing—original draft preparation, N.K. and F.Ž.; writing—review and editing, N.K., S.M., F.Ž., B.J., D.A., P.T. and N.G.; visualization, N.K., S.M. and F.Ž.; supervision, F.Ž., N.G. and B.J.; funding acquisition, F.Ž. and N.G. All authors have read and agreed to the published version of the manuscript.

Funding: This paper is funded through the EIT's HEI Initiative DEEPTECH-2M project, supported by EIT Digital, coordinated by EIT RawMaterials, funded by the European Union.

Data Availability Statement: The data that support the findings of this study are available from the corresponding author, F.Ž., upon reasonable request.

Conflicts of Interest: The authors declare no conflicts of interest.

References

1. Alexander, A.E.; Wake, N.; Chepelev, L.; Brantner, P.; Ryan, J.; Wang, K.C. A Guideline for 3D Printing Terminology in Biomedical Research Utilizing ISO/ASTM Standards. *3D Print. Med.* **2021**, *7*, 8. [CrossRef]
2. Jaisingh Sheoran, A.; Kumar, H. Fused Deposition Modeling Process Parameters Optimization and Effect on Mechanical Properties and Part Quality: Review and Reflection on Present Research. *Mater. Today Proc.* **2020**, *21*, 1659–1672. [CrossRef]
3. Huu, N.H.; Phuoc, D.P.; Huu, T.N.; Thu, H.T.T. Optimization of The FDM Parameters to Improve the Compressive Strength of the PLA-Copper Based Products. *IOP Conf. Ser. Mater. Sci. Eng.* **2019**, *530*, 012001. [CrossRef]
4. Pazhamannil, R.V.; Jishnu Namboodiri, V.N.; Govindan, P.; Edacherian, A. Property Enhancement Approaches of Fused Filament Fabrication Technology: A Review. *Polym. Eng. Sci.* **2022**, *62*, 1356–1376. [CrossRef]
5. Buj-Corral, I.; Sivatte-Adroer, M. An Experimental Investigation about the Dimensional Accuracy and the Porosity of Copper-Filled PLA Fused Filament Fabrication Parts. *Metals* **2023**, *13*, 1608. [CrossRef]
6. Mengesha Medibew, T. A Comprehensive Review on the Optimization of the Fused Deposition Modeling Process Parameter for Better Tensile Strength of PLA-Printed Parts. *Adv. Mater. Sci. Eng.* **2022**, *2022*, 1–11. [CrossRef]
7. Ahmad, M.N.; Ishak, M.R.; Mohammad Taha, M.; Mustapha, F.; Leman, Z. A Review of Natural Fiber-Based Filaments for 3D Printing: Filament Fabrication and Characterization. *Materials* **2023**, *16*, 4052. [CrossRef]
8. Dzindziora, A.; Sulowski, M.; Dzienniak, D. Application of Composite Filament with the Addition of Metallic Powders in 3D Printing. *Mater. Sci. Forum* **2023**, *1081*, 109–114. [CrossRef]
9. Vu, M.C.; Jeong, T.; Kim, J.; Choi, W.K.; Kim, D.H.; Kim, S. 3D Printing of Copper Particles and Poly(Methyl Methacrylate) Beads Containing Poly(Lactic Acid) Composites for Enhancing Thermomechanical Properties. *J. Appl. Polym. Sci.* **2021**, *138*, 49776. [CrossRef]
10. Clark, M.J.; Garg, T.; Rankin, K.E.; Bradshaw, D.; Nightingale, A.M. 3D Printed Filtration and Separation Devices with Integrated Membranes and No Post-Printing Assembly. *React. Chem. Eng.* **2024**, *9*, 251–259. [CrossRef]
11. Fijoł, N.; Mathew, A.P. Accelerated Ageing of 3D Printed Water Purification Filters Based on PLA Reinforced with Green Nanofibers. *Polym. Test.* **2023**, *129*, 108270. [CrossRef]
12. Piekarz, I.; Sorocki, J.; Wincza, K.; Gruszczynski, S.; Papapolymerou, J. Suspended Microstrip Low-Pass Filter Realized Using FDM Type 3D Printing with Conductive Copper-Based Filament. In Proceedings of the 2018 IEEE 68th Electronic Components and Technology Conference (ECTC), San Diego, CA, USA, 29 May–1 June 2018; pp. 2470–2476.

13. Avşar Aydın, E.; Torun, A.R. 3D Printed PLA/Copper Bowtie Antenna for Biomedical Imaging Applications. *Phys. Eng. Sci. Med.* **2020**, *43*, 1183–1193. [CrossRef] [PubMed]
14. Zárybnická, L.; Machová, D.; Dvořák, K. Effect of Copper or Carbon Fiber Addition to the 3D Printing of Polylactid Samples. *Mater. Test.* **2020**, *62*, 727–732. [CrossRef]
15. Ji, Q.; Wei, J.; Yi, J.; Zhang, L.; Ma, J.; Wang, Z. Study on the Static and Dynamic Mechanical Properties and Constitutive Models of 3D Printed PLA and PLA-Cu Materials. *Mater. Today Commun.* **2024**, *39*, 108690. [CrossRef]
16. Kesavarma, S.; Lee, E.H.; Samykano, M.; Kadirgama, K.; Rahman, M.M.; Sofiah, A.G.N. Flextural Properties of 3D Printed Copper-Filler Polylactic Acid (Cu-PLA). *IOP Conf. Ser. Mater. Sci. Eng.* **2020**, *788*, 012051. [CrossRef]
17. Nishal, M.; Ram Prasad, K.; Salman Dasthageer, M.; Ragunath, A.G. Significance of Additive Manufacturing amidst the Pandemic. *Mater. Today Proc.* **2023**, *72*, 2540–2546. [CrossRef] [PubMed]
18. Ahmed, W.; Al-Marzouqi, A.H.; Nazir, M.H.; Rizvi, T.A.; Zaneldin, E.; Khan, M. Comparative Experimental Investigation of Biodegradable Antimicrobial Polymer-Based Composite Produced by 3D Printing Technology Enriched with Metallic Particles. *Int. J. Mol. Sci.* **2022**, *23*, 11235. [CrossRef] [PubMed]
19. Pavan, M.V.; Balamurugan, K.; Balamurugan, P. Compressive Test Fractured Surface Analysis on PLA-Cu Composite Filament Printed at Different FDM Conditions. *IOP Conf. Ser. Mater. Sci. Eng.* **2020**, *988*, 012019. [CrossRef]
20. Ambruș, S.; Muntean, R.; Kazamer, N.; Codrean, C. Post-processing Technologies of Copper–Polylactic Acid Composites Obtained by 3D Printing Fused Deposition Modeling. *Mater. Des. Process. Commun.* **2021**, *3*, e251. [CrossRef]
21. Wang, Y.; Wang, Y.; Qiu, S.; Wang, C.; Zhang, H.; Guo, J.; Wang, S.; Ma, H. 3D-Printed Filters for Efficient Heavy Metal Removal from Water Using PLA@CS/HAP Composites. *Polymers* **2023**, *15*, 4144. [CrossRef]
22. Fu, F.; Wang, Q. Removal of Heavy Metal Ions from Wastewaters: A Review. *J. Environ. Manag.* **2011**, *92*, 407–418. [CrossRef]
23. Lehnen, A.; Hanke, S.; Schneider, M.; Radelof, C.M.L.; Perestrelo, J.; Reinicke, S.; Reifarth, M.; Taubert, A.; Arndt, K.M.; Hartlieb, M. Modification of 3D-Printed PLA Structures Using Photo-Iniferter Polymerization: Toward On-Demand Antimicrobial Water Filters. *Macromol. Rapid Commun.* **2023**, *44*, 2300408. [CrossRef]
24. Fijoł, N.; Mautner, A.; Grape, E.S.; Bacsik, Z.; Inge, A.K.; Mathew, A.P. MOF@Cell: 3D Printed Biobased Filters Anchored with a Green Metal–Organic Framework for Effluent Treatment. *J. Mater. Chem. A* **2023**, *11*, 12384–12394. [CrossRef]
25. Fijoł, N.; Aguilar-Sánchez, A.; Ruiz-Caldas, M.-X.; Redlinger-Pohn, J.; Mautner, A.; Mathew, A.P. 3D Printed Polylactic Acid (PLA) Filters Reinforced with Polysaccharide Nanofibers for Metal Ions Capture and Microplastics Separation from Water. *Chem. Eng. J.* **2023**, *457*, 141153. [CrossRef]
26. Ballóková, B.; Lázár, M.; Jasminská, N.; Molčanová, Z.; Michalik, Š.; Brestovič, T.; Živčák, J.; Saksl, K. Development and Testing of Copper Filters for Efficient Application in Half-Face Masks. *Appl. Sci.* **2022**, *12*, 6824. [CrossRef]
27. Gupta, S. Design and Model of Facemask to Inactivate the Novel Coronavirus. *Int. J. Glob. Environ. Issues* **2021**, *20*, 241. [CrossRef]
28. Michailidis, N.; Stergioudi, F.; Seventekidis, P.; Tsouknidas, A.; Sagris, D. Production of Porous Copper with High Surface Area for Efficient Water Purification. *CIRP J. Manuf. Sci. Technol.* **2016**, *13*, 85–89. [CrossRef]
29. Dinesh, K.R.; Deva, K.; Dinesh, B.R.; Pavithran, V. Water Purifier with Clogged Copper Filter. In Proceedings of the 2023 Intelligent Computing and Control for Engineering and Business Systems (ICCEBS), Chennai, India, 14 December 2023; IEEE: Chennai, India, 2023; pp. 1–5.
30. Ayub, H.; Khan, L.A.; McCarthy, E.; Ahad, I.U.; Fleischer, K.; Brabazon, D. Investigating the Morphology, Hardness, and Porosity of Copper Filters Produced via Hydraulic Pressing. *J. Mater. Res. Technol.* **2022**, *19*, 208–219. [CrossRef]
31. Ayub, H.; Khan, L.A.; McCarthy, E.; Ahad, I.U.; Sreenilayam, S.; Fleischer, K.; Brabazon, D. Investigating the Morphology, Hardness, and Porosity of Spherical and Dendritic Copper Powder Filters Produced via Cold Isostatic Pressing. In *Characterization of Minerals, Metals, and Materials 2023*; Zhang, M., Peng, Z., Li, B., Monteiro, S.N., Soman, R., Hwang, J.-Y., Kalay, Y.E., Escobedo-Diaz, J.P., Carpenter, J.S., Brown, A.D., et al., Eds.; The Minerals, Metals & Materials Series; Springer Nature Switzerland: Cham, Germany, 2023; pp. 207–218. ISBN 978-3-031-22575-8.
32. Yoo, S.; Yang, I.; Jeong, J.; Chang, J.; Kim, S. Pure Metallic Nanofibrillar Membrane for High-Performance Electrostatic Air Filtration with Antimicrobial and Reusable Characteristics. *Environ. Sci. Nano* **2023**, *10*, 2437–2447. [CrossRef]
33. Sun, X.; Dong, Z.; Cheng, K.; Chu, D.; Kong, D.; Hu, Y.; Duan, J. Fabrication of Oil–Water Separation Copper Filter by Spatial Light Modulated Femtosecond Laser. *J. Micromechanics Microengineering* **2020**, *30*, 065007. [CrossRef]
34. Khew, S.Y.; Tan, C.F.; Yan, H.; Lin, S.; Thian, E.S.; Zhou, R.; Hong, M. Nanosecond Laser Ablation for Enhanced Adhesion of CuO Nanowires on Copper Substrate and Its Application for Oil-Water Separation. *Appl. Surf. Sci.* **2019**, *465*, 995–1002. [CrossRef]
35. Wang, H.; Deng, D.; Zhai, Z.; Yao, Y. Laser-Processed Functional Surface Structures for Multi-Functional Applications-a Review. *J. Manuf. Process.* **2024**, *116*, 247–283. [CrossRef]
36. Popescu, V.; Prodan, D.; Cuc, S.; Saroşi, C.; Furtos, G.; Moldovan, A.; Carpa, R.; Bomboş, D. Antimicrobial Poly (Lactic Acid)/Copper Nanocomposites for Food Packaging Materials. *Materials* **2023**, *16*, 1415. [CrossRef]
37. Lyu, L.; Peng, H.; An, C.; Sun, H.; Yang, X.; Bi, H. An Insight into the Benefits of Substituting Polypropylene with Biodegradable Polylactic Acid Face Masks for Combating Environmental Emissions. *Sci. Total Environ.* **2023**, *905*, 167137. [CrossRef] [PubMed]
38. Pierpaoli, M.; Giosuè, C.; Czerwińska, N.; Rycewicz, M.; Wieloszyńska, A.; Bogdanowicz, R.; Ruello, M.L. Characterization and Filtration Efficiency of Sustainable PLA Fibers Obtained via a Hybrid 3D-Printed/Electrospinning Technique. *Materials* **2021**, *14*, 6766. [CrossRef]

39. Södergård, A.; Stolt, M. Properties of Lactic Acid Based Polymers and Their Correlation with Composition. *Prog. Polym. Sci.* **2002**, *27*, 1123–1163. [CrossRef]
40. *ISO 5167-1:2022*; Measurement of Fluid Flow by Means of Pressure Differential Devices Inserted in Circular Cross-Section Conduits Running Full—Part 1: General Principles and Requirements. ISO Publications: Geneva, Switzerland, 2022.
41. Açıkbaş, G.; Özcan, S.; Çalış Açıkbaş, N. Production and Characterization of a Hybrid Polymer Matrix Composite. *Polym. Compos.* **2018**, *39*, 4080–4093. [CrossRef]
42. Mastalygina, E.E.; Olkhov, A.A.; Vorontsov, N.V.; Kiselev, N.V.; Khaidarov, T.B.; Khaydarov, B.B.; Kolesnikov, E.A.; Burmistrov, I.N. Influence of Copper-Based Fillers on Structural and Mechanical Properties of Polylactic Acid Composites. *J. Compos. Sci.* **2022**, *6*, 386. [CrossRef]
43. Pinto, V.C.; Ramos, T.; Alves, S.; Xavier, J.; Tavares, P.; Moreira, P.M.G.P.; Guedes, R.M. Comparative Failure Analysis of PLA, PLA/GNP and PLA/CNT-COOH Biodegradable Nanocomposites Thin Films. *Procedia Eng.* **2015**, *114*, 635–642. [CrossRef]
44. Li, X.; Wang, Q.; Wei, S.; Lou, W.; Liang, J.; Chen, L.; Xu, L.; Zhou, Y. Microstructure and High-Temperature Mechanical Properties of Cu-W Composite Prepared by Hot Isostatic Pressing. *J. Alloys Compd.* **2024**, *970*, 172571. [CrossRef]
45. Mudakavi, D.; Sreesha, R.B.; Kumar, V.; Adinarayanappa, S.M. A Comprehensive Experimental Investigation on Mechanical Properties and Fracture Morphology of Particulate Composites via Material Extrusion-Based 3D Printing. *Results Mater.* **2022**, *16*, 100348. [CrossRef]
46. Vakharia, V.S.; Kuentz, L.; Salem, A.; Halbig, M.C.; Salem, J.A.; Singh, M. Additive Manufacturing and Characterization of Metal Particulate Reinforced Polylactic Acid (PLA) Polymer Composites. *Polymers* **2021**, *13*, 3545. [CrossRef]
47. Yilmaz, S.; Gul, O.; Eyri, B.; Karsli, N.G.; Yilmaz, T. Analyzing the Influence of Multimaterial 3D Printing and Postprocessing on Mechanical and Tribological Characteristics. *Macromol. Mater. Eng.* **2024**, *309*, 2300428. [CrossRef]
48. Butt, J.; Oxford, P.; Sadeghi-Esfahlani, S.; Ghorabian, M.; Shirvani, H. Hybrid Manufacturing and Mechanical Characterization of Cu/PLA Composites. *Arab. J. Sci. Eng.* **2020**, *45*, 9339–9356. [CrossRef]
49. Mohammadizadeh, M.; Lu, H.; Fidan, I.; Tantawi, K.; Gupta, A.; Hasanov, S.; Zhang, Z.; Alifui-Segbaya, F.; Rennie, A. Mechanical and Thermal Analyses of Metal-PLA Components Fabricated by Metal Material Extrusion. *Inventions* **2020**, *5*, 44. [CrossRef]
50. Török, J.; Törökova, M.; Duplakova, D.; Murcinkova, Z.; Duplak, J.; Kascak, J.; Karkova, M. Advanced Configuration Parameters of Post Processor Influencing Tensile Testing PLA and Add-Mixtures in Polymer Matrix in the Process of FDM Technology. *Appl. Sci.* **2021**, *11*, 6212. [CrossRef]
51. Butt, J.; Bhaskar, R. Investigating the Effects of Annealing on the Mechanical Properties of FFF-Printed Thermoplastics. *J. Manuf. Mater. Process.* **2020**, *4*, 38. [CrossRef]
52. Thumsorn, S.; Prasong, W.; Kurose, T.; Ishigami, A.; Kobayashi, Y.; Ito, H. Rheological Behavior and Dynamic Mechanical Properties for Interpretation of Layer Adhesion in FDM 3D Printing. *Polymers* **2022**, *14*, 2721. [CrossRef]
53. Jabbar Khan, A.; Mateen, A.; Khan, S.; He, L.; Wang, W.; Numan, A.; Peng, K.; Ahmed Malik, I.; Hussain, I.; Zhao, G. 3D Printed Micro-Electrochemical Energy Storage Devices. *Batter. Supercaps* **2023**, *6*, e202300190. [CrossRef]
54. Chen, Y.; Wu, C.; Wei, X.; Meng, X.; Liu, J.; Wang, Q. Morphology Analysis and Process Optimization of Micro-Cylinder Structure in Micro-Nano Additive Manufacturing. *J. Mech. Eng.* **2023**, *59*, 286. [CrossRef]
55. Peng, S.; Sun, S.; Zhu, Y.; Qiu, J.; Yang, H. Colourful 3D Anti-Counterfeiting Label Using Nanoscale Additive Manufacturing. *Virtual Phys. Prototyp.* **2023**, *18*, e2179929. [CrossRef]
56. Jayasinghe, S.N. Electrospray Printing: Unravelling the History of a Support Free Three-Dimensional Additive Manufacturing Technology. *Mater. Today* **2023**, *62*, 14–20. [CrossRef]
57. Menétrey, M.; Koch, L.; Sologubenko, A.; Gerstl, S.; Spolenak, R.; Reiser, A. Targeted Additive Micromodulation of Grain Size in Nanocrystalline Copper Nanostructures by Electrohydrodynamic Redox 3D Printing. *Small* **2022**, *18*, 2205302. [CrossRef] [PubMed]
58. Song, P.; Zhou, C.; Fan, H.; Zhang, B.; Pei, X.; Fan, Y.; Jiang, Q.; Bao, R.; Yang, Q.; Dong, Z.; et al. Novel 3D Porous Biocomposite Scaffolds Fabricated by Fused Deposition Modeling and Gas Foaming Combined Technology. *Compos. Part B Eng.* **2018**, *152*, 151–159. [CrossRef]